Proceedings of the 4th International Conference on Functional Materials and Civil Engineering
DOI: 10.54254/2755-2721/2026.34250

Joint Optimization of Tilt Angle and Capacity Ratio for Large-Scale Centralized Photovoltaic Power Plants in Desert Areas

Zihan Su

School of Engineering, China University of Petroleum-Beijing at Karamay, Karamay, China
2023016459@st.cupk.edu.cn

Abstract. Desert areas like Karamay in Xinjiang have high surface albedo, frequent dust storms, and extreme summer heat. These conditions make photovoltaic plant design different from conventional sites. This work investigates the optimal tilt angle and capacity ratio for a 100 MW fixed-tilt bifacial PV plant in such an environment. The electrical configuration follows IEC standards. Fifty-seven simulation scenarios covering a broad range of tilt angles and capacity ratios are run in PVsyst 7.4. The analysis focuses on in-plane irradiation, annual grid-connected energy, and levelized cost of electricity. The results show a flat-bottomed optimum region defined by a tilt angle of 36° to 37° and a capacity ratio of 1.20 to 1.25. The minimum LCOE is about 0.1842 yuan/kWh, roughly 1.3% lower than a conventional design. The high desert albedo shifts the optimal tilt approximately 9° below the local latitude, while the rear-side gain of bifacial modules contributes an extra 8% to 12% of energy yield. These findings provide a quantitative basis for customizing large-scale PV plants in similar desert and Gobi regions.

Keywords: Photovoltaic power station, Bifacial PV plant, Tilt angle, Capacity ratio, LCOE, Desert area

1. Introduction

Solar photovoltaics have become a key pillar of the global transition toward carbon neutrality [1]. Global installed capacity grew from about 0.1 GW in 1992 to over 500 GW by 2018, and in 2023 solar energy was the largest contributor to new power capacity worldwide [2]. In China, large-scale PV bases under the "14th Five-Year Plan" and the dual-carbon strategy are now concentrated in western regions with abundant solar resources, where desert areas offer both high irradiation and vast available land [3]. However, such sites also bring unique design challenges. Karamay in Xinjiang, located at 45.54°N 84.77°E in the Junggar Basin, has a typical temperate desert climate: 2600–2800 sunshine hours per year, winter lows below −40 °C, and summer highs above 40 °C. The ground surface albedo here ranges from 0.20 to 0.30, much higher than that of grassland or bare soil which is normally 0.10–0.15, and frequent dust storms in winter and spring cause heavy soiling on modules. These climatic and technical factors together mean that desert PV plants cannot be designed using conventional rules developed for temperate or grassland environments.

© 2026 The Authors. This is an open access article distributed under the terms of the Creative Commons Attribution License 4.0 (https://creativecommons.org/licenses/by/4.0/).

DOI: 10.54254/2755-2721/2026.34250

Large-scale centralized grid-connected PV plants have clear advantages over other configurations: higher land-use efficiency than distributed systems, fewer inverters and lower upfront cost than string-inverter architectures, and no battery storage costs thanks to direct grid integration [4]. Two design parameters are fundamental to energy yield and economic performance: the tilt angle of modules and the system capacity ratio, or DC/AC ratio. Tilt angle determines the in-plane irradiation received. Yuan showed that module orientation and tilt angle strongly affect output power [5], and Xiao et al. developed an empirical formula for tilt-angle optimization in mountainous terrain [6]. Many studies in different climates have examined how tilt angle influences energy yield and system efficiency [7-9]. The capacity ratio compares installed DC power to nominal AC inverter power and affects inverter utilization, system cost, and grid-connected output. Wang et al. found that moderate oversizing can improve utilization and shorten payback periods, although excessive oversizing increases losses and capital cost [10]. Chen et al., Kratzenberg et al., and Good & Jeremiah further confirmed the strong impact of capacity ratio on plant performance and economic viability [11-13].

However, existing research has several shortcomings. Most tilt-angle optimization studies focus on conventional settings such as grassland, urban rooftops or mountains, with few addressing desert climates where high albedo fundamentally changes the radiative environment. Capacity ratio optimization has usually been done independently of tilt angle, and the interaction between the two parameters has rarely been explored jointly. Moreover, systematic simulations that combine bifacial module characteristics, desert-specific albedo in the range of 0.20–0.30 and levelized cost of electricity as a unified economic criterion are still scarce. To address these gaps, this study takes a 100 MW fixed-tilt bifacial PV plant in the Karamay desert as a reference. The electrical design including series and parallel module counts and the number of inverters is first performed using IEC standard formulas. Then 47 scenarios covering 14 tilt angles from 33° to 50.5° and 7 capacity ratios from 1.00 to 1.30 are simulated in PVsyst 7.4. Desert-specific parameters—albedo 0.25, annual soiling loss 4.0 %, and N-type module temperature coefficients—are explicitly included. Using levelized cost of electricity as the core metric, the joint influence of tilt and capacity ratio on energy yield, system efficiency and economics is analyzed. The objectives are to find the tilt-ratio combination that minimizes LCOE, to quantify how desert environmental parameters reshape the optimal design, and to provide quantitative guidance for large-scale PV plants in similar desert and Gobi regions.

2. Research methods and model establishment

2.1. Electrical design based on IEC standards

Before running the simulations worked out the electrical configuration of the plant based on Karamay's climate conditions. Tables 1, table 2 and table 3 list the main climate parameters, the selected PV module specifications, and the inverter specifications.

Table 1. Climate parameters of the Karamay site

Parameter	Value
Extreme high temperature (t')	49.1°
Extreme low temperature (t)	-42°

DOI: 10.54254/2755-2721/2026.34250

Table 2. PV module specifications

Parameter	Value
Module model	Longi_LR5-72HBD 545 M G2 Bifacial.PAN
Maximum power point voltage (Ump)	41.8V
Open-circuit voltage (UOC)	49,65V
Temperature coefficient of Ump ($K_V^{'}$)	-0.33%/°C
Temperature coefficient of UOC (Kv)	-0.24%/°C
Rated power (P)	545.0Wp

Table 3. Inverter specifications

Parameter	Value
Inverter model	Sungrow_SG250_HX.OND
Maximum MPPT voltage (Umpptmax)	1450V
Minimum MPPT voltage (Umpptmin)	500V
Maximum DC input voltage (UDCmax)	1500V
Maximum AC output power (Pmax)	250kVAC
Maximum number of DC inputs	24

The number of PV modules connected in series, N, must simultaneously satisfy two constraints: the string voltage must remain within the inverter's MPPT operating range under all temperature conditions, and the open-circuit voltage must never exceed the inverter's maximum DC input voltage. The number of parallel strings per inverter, N′, is governed by the inverter's maximum AC output power and the chosen capacity ratio. These constraints are expressed through Eqs. (1)–(3), derived from IEC standards.

$$\frac{U_{mpptmin}}{U_{mp}[1+(t^{'}-25)K_V^{'}]} \leq N \leq \frac{U_{mpptmax}}{U_{mp}[1+(t-25)K_V^{'}]} \tag{1}$$

$$N \leq \frac{U_{DCmax}}{U_{OC}[1+(t-25)K_V]} \tag{2}$$

$$N^{'} = \frac{P_{max} \times Capacity\ Ratio}{N \times P} \tag{3}$$

Equation (1) constrains the string operating voltage to remain within the inverter MPPT voltage range under all expected temperature conditions. At the extreme high temperature of 49.1 °C, the module operating voltage reaches its minimum; the lower bound of Eq. (1) ensures that even under this condition the string voltage remains sufficient for MPPT tracking. At the extreme low temperature of −42 °C, the module voltage rises to its maximum, and the upper bound of Eq. (1) prevents the string voltage from exceeding the inverter's MPPT ceiling. Equation (2) provides an independent safety constraint: at −42 °C, the open-circuit voltage must not surpass the inverter's maximum DC input voltage, thereby protecting the power electronics from irreversible damage. Solving Eq. (1) and (2) together yields the feasible series module count $13 \leq N \leq 26$. To minimize the number of parallel connections—thus reducing cabling cost and potential failure points—N = 26 was

DOI: 10.54254/2755-2721/2026.34250

selected; the resulting higher string voltage also reduces DC-side ohmic losses. With N fixed at 26, the number of parallel strings per inverter for each capacity ratio was obtained from Eq. (3).

With N and N′ determined, the total number of inverters N_{INV} is fixed by the required AC-side capacity of 100.1 MW and calculated using Eq. (4). The total number of PV modulesN_{PV} is then obtained from Eq. (5) and varies with the capacity ratio across the range 1.00–1.30. The number of DC input channels utilized per inverter is given by Eq. (6) and must not exceed the inverter's maximum of 24 inputs. The resulting electrical configuration for each capacity ratio is summarized in Table 4.

$$N_{INV} = \frac{100100000}{P_{MAX}} \tag{4}$$

$$N_{PV} = N \times N^{'} \times N_{INV} \tag{5}$$

$$Input\ channels = \frac{N^{'}}{N_{INV}} \tag{6}$$

Table 4. Electrical configuration for each capacity ratio

Capacity ratio	N_{INV}	N_{PV}	DC inputs per inverter
1.00	400	183508	18
1.05	400	192686	19
1.10	400	201838	20
1.15	400	211016	21
1.20	400	220194	22
1.25	400	229372	23
1.30	400	238550	23

2.2. Simulation platform and meteorological data

All simulations were performed using PVsyst 7.4, a widely adopted software platform for PV system design, energy yield prediction, and performance evaluation [14]. The software models PV modules using a single-diode equivalent circuit model. For bifacial modules, the rear-side irradiance is calculated via the view-factor method and converted to electrical output using a bifaciality efficiency factor, following the approach of Shao et al. [15]. The simulation operates on an hourly energy balance basis, resolving in-plane irradiance, module temperature, inverter maximum power point tracking (MPPT), and all major system losses. This level of temporal resolution and physical detail makes PVsyst well-suited for capturing the effects of the desert environment, particularly the influence of high ground reflectance on rear-side irradiance.

Meteorological input data were obtained from the Meteonorm 8.1 global database, which synthesizes typical meteorological year (TMY) data from long-term ground station observations and satellite remote sensing retrievals using stochastic time-series generation. The TMY dataset for the Karamay site (45.54°N, 84.77°E) was used, providing hourly time series of global horizontal irradiance, diffuse horizontal irradiance, ambient temperature, wind speed and direction, and ground albedo. The annual global horizontal irradiation at the site is 1465 kWh/m², with a diffuse fraction of

DOI: 10.54254/2755-2721/2026.34250

approximately 28%, consistent with the radiative climate characteristics of the southern Junggar Basin.

2.3. Desert-specific environmental parameters

The desert environment of Karamay imposes several site-specific influences on plant performance that must be explicitly incorporated into the simulation. The key environmental parameters used in this study are listed in Table 5, and their rationale is discussed below.

Table 5. Key environmental parameters adopted in the simulation

Parameter	Value	Basis
Ground reflectance (albedo)	0.25	Median of measured desert sand range (0.20–0.30)
Annual soiling loss	4.0%	Annual average estimated from regional dust storm frequency
Module temperature coefficient (Pmp)	-0.24%/°C	Manufacturer specification for N-type modules
Bifacial rear-side gain	Calculated by PVsyst	View-factor model with site albedo

Ground reflectance was set to 0.25, the median of the measured range for desert sand (0.20–0.30). This value is substantially higher than that of typical grassland or bare soil environments (~0.10–0.15). The elevated albedo enhances the reflected irradiance received by the rear side of bifacial modules, which in turn affects the optimal tilt angle—a lower tilt allows the rear surface to capture a larger fraction of ground-reflected radiation.

Annual soiling loss was set to 4.0%, reflecting the frequent dust events in winter and spring in Karamay. Dust accumulation on the module surface reduces the transmittance of the glass cover, weakening the solar irradiance reaching the cells. The 4.0% value represents an annualized estimate based on regional dust storm frequency and is consistent with soiling rates reported for arid and semi-arid regions.

Module temperature coefficient was taken as −0.24%/°C, corresponding to the manufacturer-specified value for the LR5-72HBD bifacial modules. Owing to the lower temperature coefficient of N-type cells compared to conventional P-type technologies, the power loss induced by high ambient temperatures in summer is partially mitigated—an important advantage in desert climates where module operating temperatures frequently exceed 45 °C.

2.4. Simulation scenarios

To systematically investigate the joint effect of tilt angle and capacity ratio on plant performance and economic viability, a full-factorial simulation scheme was designed. All scenarios assume a south-facing fixed-tilt orientation. The tilt angle was varied from 33°to 50.5°, with finer sampling steps (2.5°) around two regions of interest: the local latitude (45.5°) and the theoretical peak of annual in-plane irradiation (33°–38°). The capacity ratio was set from 1.00 to 1.30 with a step of 0.05. This covers the whole range from conservative designs with no DC oversizing up to the moderate and high oversizing levels often used in today's utility-scale projects. In total, 14 tilt angles and 7 capacity ratios were combined, giving 47 independent simulation scenarios.

For each scenario we recorded annual in-plane irradiation, annual grid-connected energy, performance ratio PR, and capacity factor. The levelized cost of electricity LCOE was used as the

DOI: 10.54254/2755-2721/2026.34250

primary economic metric. LCOE consolidates all capital and operating costs over the plant lifetime into a single cost per unit of energy [16, 17]. Therefore, LCOE was adopted as the core criterion to compare the economic performance of different tilt and capacity ratio combinations.

2.5. Economic evaluation model

The levelized cost of electricity (LCOE) was adopted as the unified economic benchmark for comparing alternative design configurations. LCOE is defined as the ratio of total life-cycle costs to total lifetime electricity production, as expressed in Eq. (7)

$$LCOE = \frac{(C_{inv} + \sum_{t=1}^{n} C_{O\&M,t})}{\sum_{t=1}^{n} E_t} \quad (7)$$

Where C_{inv} is the total initial investment, $C_{O\&M,t}$ is the operation and maintenance (O&M) cost in year(t), E_t is the grid-connected electricity generated in year(t), and n= 25 years is the plant lifetime.

Table 6. Initial investment cost assumptions

Cost item	Unit cost
PV module	400 yuan/piece
Inverter	43,000 yuan/unit
Balance of system (mounting structure, cabling, civil works, etc.)	2.47 yuan/ Wp
Substation and grid connection	0.5 yuan/ Wp

The cost assumptions are listed in Table 6. PV module cost was applied per unit, inverter cost per unit, and balance-of-system (BOS) costs—including mounting structures, cabling, and civil works—were scaled by the DC-side installed capacity at 2.47 yuan/ Wp. Substation and grid connection costs were similarly scaled by DC capacity at 0.50 yuan/ Wp. The total initial investmentC_{inv} thus varies with both the number of modules (a function of capacity ratio) and the total DC capacity. The annual O&M cost was assumed constant over the 25-year operational lifetime and was calculated by multiplying the DC capacity by 0.04 yuan/ Wp /year.

The annual electricity yieldE_t accounts for module degradation over the plant lifetime. A first-year degradation rate of 1.5% was applied, followed by an annual degradation rate of 0.55% from year 2 to year 25. The annual energy output E_t was calculated according to this piecewise degradation schedule, and the total lifetime generation was obtained by summation. This model captures the simultaneous effects of tilt angle and capacity ratio on initial investment, long-term O&M costs, and total energy revenue, thereby providing a consistent economic basis for the comparative analysis of all simulation scenarios.

3. Results and analysis

3.1. Determination of optimal tilt angle

Figure 1 shows how annual in-plane irradiation changes with tilt angle from 33° to 50.5°. The curve has a single peak near 37°. This matches the 35.5°–40.5° range predicted by the IEA empirical formula shown in Eq. (8), which confirms that the radiation model works well.

DOI: 10.54254/2755-2721/2026.34250

$$\beta = \varphi \pm (5^{\circ} \sim 10^{\circ}) \tag{8}$$

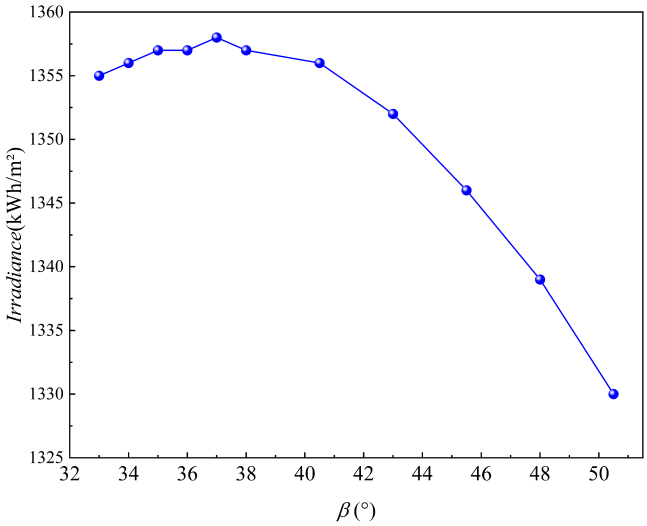

Figure 1. Annual in-plane irradiation (GTI) as a function of tilt angle(picture credit : original)

But getting the most irradiation does not always mean the lowest LCOE. Figure 2 and figure 3 show how annual grid-connected energy, performance ratio, and LCOE change with tilt angle across different capacity ratios. Each LCOE curve drops first as tilt angle rises, then hits a low point, and finally climbs back up. Interestingly, the curves have a fairly flat bottom near the low point. Over tilt angles from 34° to 39°, LCOE changes by less than 0.2%. That means the economic optimum is actually a range of tilt angles rather than a single number. The region with the lowest LCOE falls close to the GTI peak around 37°, but sits a little lower, roughly from 36° to 37°.

The main reason why does the optimal tilt shift downward is the high ground reflectance in the Karamay desert. With albedo at 0.25, the back side of bifacial modules picks up a lot of reflected light from the ground. A tilt a bit lower than the local latitude cuts down the direct front-side radiation, but the back side sees more ground reflection and more than makes up for the loss. So total in-plane irradiation goes up, and so does annual energy output. Also, a lower tilt angle slightly reduces the amount of material needed for the mounting structure, which helps a little on the cost side. Taking both energy gain and cost savings together, the best tilt range for the Karamay desert comes out as 36° to 37°. That is about 9° lower than the local latitude of 45.5°, which is quite different from the common rule that tilt should be roughly equal to latitude. This shows that desert surface reflectance has a strong effect on choosing module orientation. And because the LCOE bottom is flat, designers have some flexibility to adjust tilt within this range to meet other site constraints without hurting economics.

DOI: 10.54254/2755-2721/2026.34250

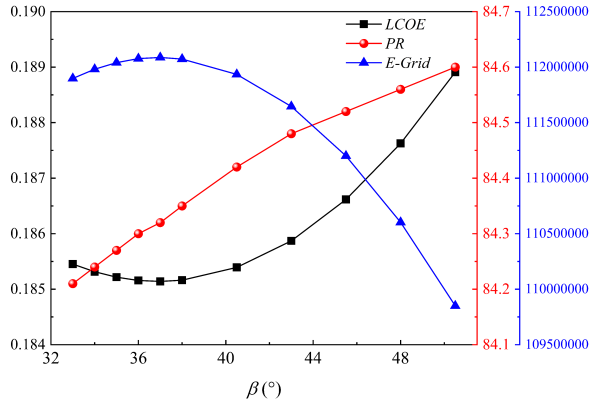

Figure 2. Performance ratio (PR) and annual grid-connected energy (E_Grid) as a function of tilt angle(picture credit : original)

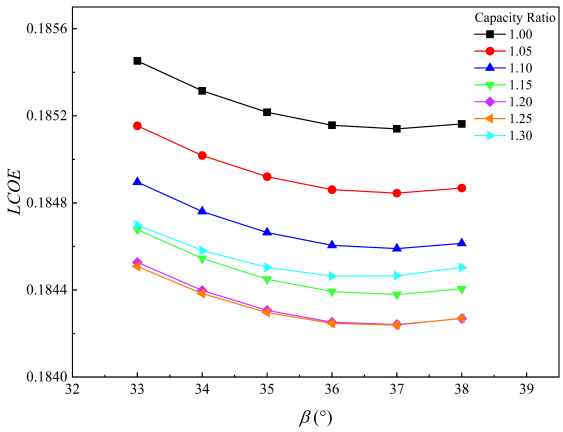

Figure 3. LCOE as a function of tilt angle under different capacity ratios(picture credit : original)

3.2. Determination of optimal capacity ratio range

If keep the tilt angle fixed, raising the capacity ratio means adding more DC power than the inverter can handle at peak times. This lets the plant use more of the available sunlight, especially during low-light hours. Figure 4 and figure 5 show how annual grid-connected energy, performance ratio, and inverter overload loss change with the capacity ratio. As the ratio goes from 1.00 to 1.30, E-Grid keeps rising but the gain gets smaller each step. Once the ratio passes about 1.20, the inverter starts clipping power for more hours each day. The overload loss—energy that the modules could produce but the inverter cannot convert—goes up sharply.

Raising the capacity ratio also causes the performance ratio to drop a little. The reason is straightforward. When the inverter is oversize on the DC side, it hits its power ceiling more often around noon. Any DC power above that limit cannot be turned into AC output, so the system's nominal efficiency goes down. That said, the drop is small—less than one percentage point across the whole range from 1.00 to 1.30. So moderate oversizing does not really harm system efficiency in a meaningful way.

If look at how LCOE changes with capacity ratio, the curve is U-shaped. For a given tilt angle, LCOE first drops as the ratio rises, reaches a low point, and then climbs back up. On the cost side, adding more modules increases the upfront investment and also pushes up annual operation and maintenance costs because both are tied to DC capacity. On the revenue side, total electricity output keeps increasing, but each extra unit of DC capacity brings a smaller gain. Once the ratio goes above about 1.20, the additional energy from the extra modules no longer pays for the added cost. The low point of the LCOE curve is fairly flat, meaning that LCOE changes by less than 0.3% when the ratio moves from 1.15 to 1.25. So the economic optimum is actually a range rather than a single value. Considering both cost and revenue, the best capacity ratio range is 1.20 to 1.25, with 1.20 giving the lowest LCOE for most tilt angles.

DOI: 10.54254/2755-2721/2026.34250

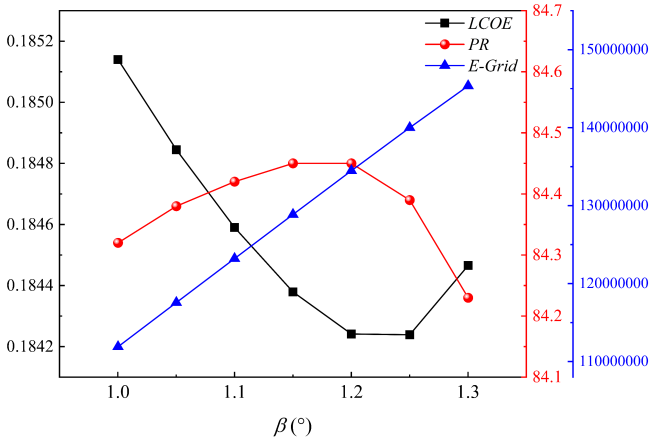

Figure 4. Annual grid-connected energy (E_Grid) and performance ratio (PR) as a function of capacity ratio(picture credit : original)

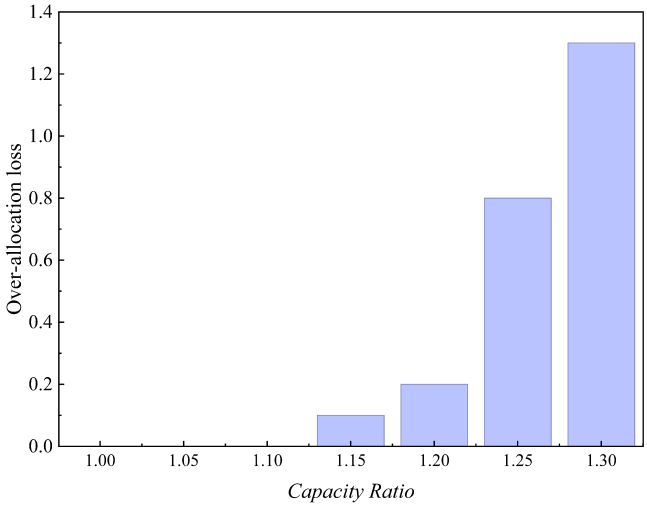

Figure 5. Over-allocation loss as a function of capacity ratio(picture credit : original)

3.3. Joint optimization of tilt angle and capacity ratio

Table 7 compares four candidate setups inside the optimal range and also shows the conventional reference design with a tilt of 45.5° and a capacity ratio of 1.00. Among the candidates, the 37° tilt and 1.20 ratio gives the highest annual grid-connected energy, about 140.21 GWh per year. The two 36° cases produce roughly 134.68 GWh per year, about 3.9% less. But energy yield by itself does not decide what is best economically.

Take the four candidate combinations as an example. For 36° with a capacity ratio of 1.20, LCOE is 0.18425 yuan/kWh; for 36° with 1.25 it is 0.18424; for 37° with 1.20 it is 0.18425; and for 37° with 1.25 it is 0.18424. The largest difference among these values is only about one ten-thousandth of a yuan, which is negligible in both engineering and economic terms. This means the LCOE surface is nearly flat over the rectangle defined by tilt angles from 36° to 37° and capacity ratios from 1.20 to 1.25. In other words, the parameter space contains a flat-bottomed valley.

The performance ratio of these four combinations stays between 84.37% and 84.45%. If we raise the capacity ratio from 1.20 to 1.25 while keeping the same tilt angle, the PR changes by less than

DOI: 10.54254/2755-2721/2026.34250

0.05 percentage points. That is a very small shift. So moderate DC oversizing within this range does not really hurt system efficiency.

The capacity factor of the 37° setups is about 0.1600, higher than the 0.1538 seen at 36°. The steeper tilt captures more in-plane irradiation, which explains the difference. For comparison, the conventional reference design with a tilt of 45.5° and a capacity ratio of 1.00 produces only 111.20 GWh per year. That is roughly 20.7% lower than the best candidate here. Its LCOE is 0.18662 yuan/kWh, about 1.3% higher than the optimal. Over a 25-year lifetime, that 1.3% difference in LCOE adds up to a lot of saved cost for a 100 MW plant..

Table 7. Tilt angle and capacity ratio combinations

	36° 1.2	36° 1.25	37° 1.2	37° 1.2	45.5° 1.0 (Best in theory)
Inclined plane irradiation volume (kWh/m²)	1357	1357	1358	1358	1346
E_Grid (kWh/yr)	134679932	134687954	140201170	140207120	111200094
PR(%)	84.42	84.45	84.37	84.39	84.52
Array MPPT Power output (kWh)	138710254	138724437	144491895	144506669	114716565
Capacity factor	0.153744215	0.153753372	0.160046998	0.16005379	0.126940747
Quantity of series components	26	26	26	26	26
Quantity of parallel components	8469	8469	8822	8822	7058
LCOE	0.184252137	0.184241163	0.184246606	0.184238787	0.186616913

Figures 6 ,figure 7 figure 8 and figure 9 show how LCOE changes across tilt angle and capacity ratio. In the heatmap of Figure 10, a dark shaded minimum appears in the rectangle from 36° to 37° tilt and 1.20 to 1.25 capacity ratio. Outside that rectangle, the color gets lighter. LCOE rises faster when we move away in tilt angle than when we move away in capacity ratio. Figure 11, the contour map, tells the same story. Contour lines are far apart inside the optimal region, which means LCOE does not change much there. They become crowded when capacity ratio drops below 1.10 or tilt goes above 45°, showing that LCOE becomes very sensitive to parameter changes in those outer areas. Figure 12 gives a three-dimensional view. The surface curves downward like a concave dish and has a flat-bottomed valley in the 36°–37°, 1.20–1.25 rectangle. The surface is steeper along the tilt direction than along the capacity ratio direction. So moving away from the optimal tilt raises LCOE more than moving away from the optimal capacity ratio. If we push tilt up to 45.5° or cut capacity ratio down to 1.00, the surface rises a lot, and we cannot get back to the global minimum even by keeping the other parameter at its best value.

DOI: 10.54254/2755-2721/2026.34250

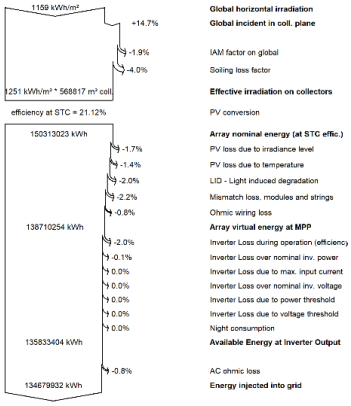

Figure 6. Loss diagram for tilt angle 36°, capacity ratio 1.20(picture credit : original)

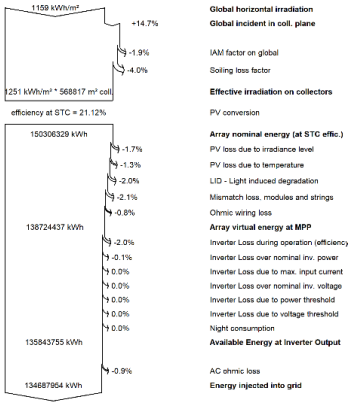

Figure 7. Loss diagram for tilt angle 37°, capacity ratio 1.20(picture credit : original)

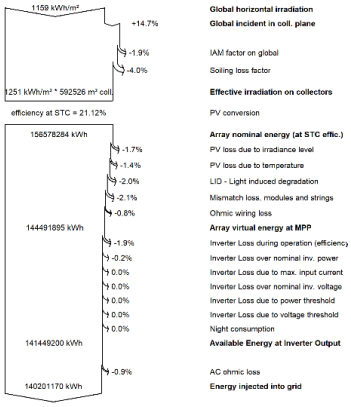

Figure 8. Loss diagram for tilt angle 36°, capacity ratio 1.25(picture credit : original)

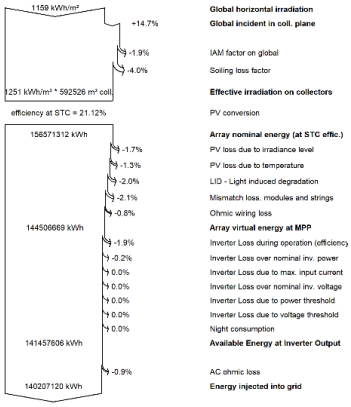

Figure 9. Loss diagram for tilt angle 37°, capacity ratio 1.25(picture credit : original)

Figures 10 to 12 show how LCOE changes across tilt angle and capacity ratio. In the heatmap of Figure 10, a dark shaded minimum appears in the rectangle from 36° to 37° tilt and 1.20 to 1.25 capacity ratio. Outside that rectangle the color gets lighter. LCOE rises faster when we move away in tilt angle than when we move away in capacity ratio. The contour map in Figure 11 confirms the same pattern. Inside the optimal region the contour lines are far apart, which means LCOE does not change much there. When capacity ratio drops below 1.10 or tilt goes above 45°, the contour lines become crowded, so LCOE becomes very sensitive to parameter changes in those outer ranges. The three-dimensional surface plot in Figure 12 backs up these observations. The surface is concave and has a flat-bottomed valley in the 36°–37°, 1.20–1.25 rectangle. The surface curvature is steeper along the tilt direction than along the capacity ratio direction. That tells us LCOE responds more strongly to a deviation in tilt angle than to a deviation in capacity ratio. If we push tilt up to 45.5° or cut capacity ratio down to 1.00, the surface rises sharply and we cannot get back to the global minimum even if we keep the other parameter at its best value.

In summary, the joint optimization gives a flat-bottomed economic optimum for the 100 MW plant in the Karamay desert. The best design lies in a rectangular region where tilt angle is between

DOI: 10.54254/2755-2721/2026.34250

36° and 37° and capacity ratio is between 1.20 and 1.25. Inside this region, LCOE stays around 0.1842 yuan/kWh, which is about 1.3% lower than that of the conventional reference design. Because the bottom is flat, designers have a flexible window. They can adjust tilt angle and capacity ratio within this range to meet site-specific needs like land area, mounting structure cost, or inverter availability without noticeably changing the levelized cost of electricity.

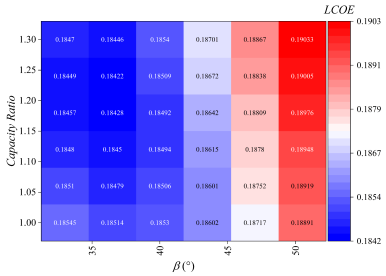

Figure 10. Heatmap of LCOE distribution under combined variation of tilt angle and capacity ratio(picture credit : original)

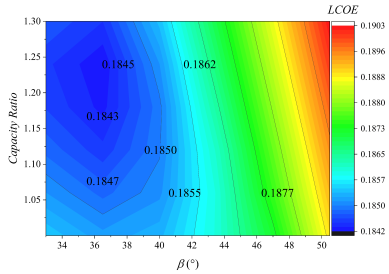

Figure 11. Contour map of LCOE in the tilt angle–capacity ratio plane(picture credit : original)

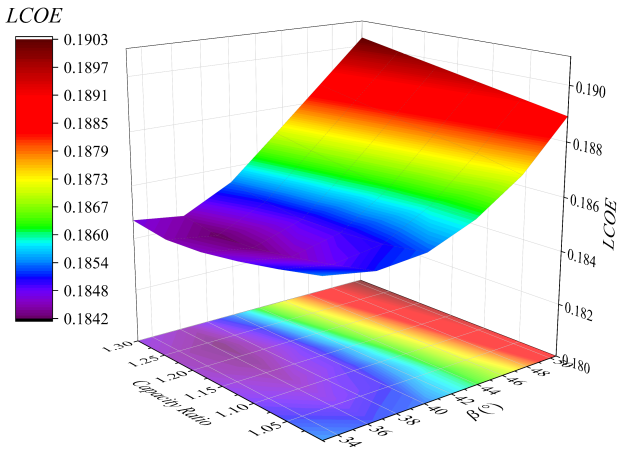

Figure 12. Joint optimization surface of LCOE with respect to tilt angle and capacity ratio(picture credit : original)

4. Discussion

4.1. Influence of desert environment on optimal design parameters

The optimal tilt range found in this study is 36° to 37°, which lies about 9° below the local latitude of 45.5°. The main reason is the high ground reflectance in the desert. In conventional environments like grassland or bare soil, ground albedo is typically between 0.10 and 0.15. Under those conditions, the rear-side gain of bifacial modules is limited, and the optimal tilt is largely determined by front-side beam radiation, thus staying close to the local latitude. In the Karamay desert, however, the albedo reaches 0.25, which significantly increases the reflected radiation reaching the rear side of the modules. A lower tilt angle reduces the front-side beam component, but the reduction is more than compensated by the higher rear-side view factor to the ground. The net effect is a

DOI: 10.54254/2755-2721/2026.34250

higher total in-plane irradiation and a shift of the economic optimum to tilt angles well below the latitude.

The desert radiative environment also affects the optimal capacity ratio. High albedo pushes up in-plane irradiation all year round and stretches the high-irradiance period, especially in spring, autumn and winter. That makes a higher capacity ratio worthwhile because the plant can harvest more of that extra resource. On top of that, N-type modules have a low temperature coefficient, about −0.24%/°C. In summer, module operating temperature often goes above 45°C, and this low coefficient reduces the power loss at peak hours. So oversizing does not eat away the economic gain as much as it would with other module types. Because of the higher irradiation and better thermal behavior, the best capacity ratio ends up being higher than what you would see in grassland or bare-soil locations, and that pushes LCOE down.

4.2. Comparison with previous studies, limitations and contributions

The optimal tilt range of 36°–37° found here lies about 9° below the local latitude. In non-desert environments with typical albedo of 0.10–0.15, previous studies generally report optimal tilts within ±5° of the latitude [5-8]. The larger downward shift observed in this work is thus directly attributable to the high desert albedo, which amplifies the rear-side gain of bifacial modules. Likewise, the optimal capacity ratio range of 1.20–1.25 is notably higher than the 1.05–1.15 typical for conventional sites [10-13]. Two desert-specific factors explain this: the elevated in-plane irradiation due to high albedo broadens the high-irradiance window, and the low temperature coefficient of N-type modules (−0.24%/°C) keeps clipping losses acceptable even at higher oversizing levels.

Two limitations should be noted. Soiling loss and ground reflectance were treated as annual averages, ignoring seasonal variability, and the economic model used static cost parameters without incorporating price or interest rate uncertainties.

The main contributions of this study are twofold. First, it quantifies the joint effect of tilt angle and capacity ratio on LCOE for a utility-scale bifacial PV plant in a desert environment—a combination rarely addressed in the literature—and identifies a flat-bottomed optimum region rather than a single point. Second, it clarifies the underlying mechanism: high desert albedo shifts the optimal tilt substantially below the latitude and simultaneously supports a higher economically optimal capacity ratio, challenging the conventional rule-of-thumb that sets tilt approximately equal to latitude.

5. Conclusion

This study optimized tilt angle and capacity ratio for a 100 MW fixed-tilt bifacial PV plant in the Karamay desert. Electrical design followed IEC standards, and 47 scenarios covering 14 tilt angles from 33° to 50.5° and 7 capacity ratios from 1.00 to 1.30 were simulated in PVsyst 7.4. The joint economic optimum is a flat-bottomed region with tilt of 36°–37° and capacity ratio of 1.20–1.25. In this region, LCOE is about 0.1842 yuan/kWh, roughly 1.3% lower than the conventional design of 45.5° tilt and 1.00 capacity ratio. The high desert albedo of 0.25 brings the optimal tilt down by about 9° from the local latitude, because the rear-side gain of bifacial modules becomes stronger and reduces the weight of front-side beam radiation. Meanwhile, the higher in-plane irradiation and the low temperature coefficient of N-type modules allow a higher optimal capacity ratio than what is typical for grassland or bare-soil sites. Across the optimal region, performance ratio stays within 84.4% to 84.5%, showing that moderate oversizing does not meaningfully harm system efficiency.

DOI: 10.54254/2755-2721/2026.34250

The flat-bottomed optimum gives designers a flexible window: tilt and capacity ratio can be adjusted to meet site-specific needs without noticeably changing LCOE. In summary, desert environments systematically lower the optimal tilt and moderately raise the optimal capacity ratio. The LCOE-minimization framework presented here offers a quantitative basis for designing large-scale PV plants in similar desert and Gobi regions.

References

[1] Ding, M., Wang, W., Wang, X., Song, Y., Chen, D., & Sun, M. (2014). A review on the effect of large-scale PV generation on power systems. Proceedings of the CSEE, 34(1), 1.
[2] Zhao, Y., Li, Z., Gao, X., et al. (2021). Characteristics of surface fluxes over a large-scale Gobi photovoltaic power station on clear summer days. Acta Energiae Solaris Sinica, 42(1), 138.
[3] Hayinaer, T., Gao, L., Wei, L., et al. (2025). Intelligent design method for large-scale photovoltaic power stations in desert areas based on particle swarm optimization. Xinjiang Petroleum & Natural Gas, 21(1), 81.
[4] Zhao, Z., Lei, Y., He, F., et al. (2011). Overview of large-scale grid-connected photovoltaic power plants. Automation of Electric Power Systems, 35(1), 101.
[5] Yuan, P. (2025). Influence of photovoltaic array layout on electrical output in photovoltaic power stations. Light Sources and Illumination, (1), 129.
[6] Xiao, Y., Zhang, M., Guo, Z., et al. (2020). Optimization method for installation angle of fixed photovoltaic modules in mountainous photovoltaic power stations. Acta Energiae Solaris Sinica, 41(5), 329.
[7] Wu, Z., Xu, Z., Hu, X., et al. (2016). Study on practical calculation model of solar irradiance on inclined surfaces. Acta Energiae Solaris Sinica, 37(3), 787.
[8] Li, F., Zhao, J., Duan, S., et al. (2015). Evaluation of three monthly average total radiation models for inclined surfaces and study on optimal tilt angle of photovoltaic arrays. Acta Energiae Solaris Sinica, 36(2), 502.
[9] Demain, C., Journée, M., & Bertrand, C. (2013). Evaluation of different models to estimate the global solar radiation on inclined surfaces. Renewable Energy, 50, 710–713.
[10] Wang, L., Shi, J., Wu, Y., et al. (2021). Research on optimal capacity ratio of PV modules and inverters based on photovoltaic system reliability. Acta Energiae Solaris Sinica, 42(2), 498.
[11] Chen, S., Li, P., Brady, D., & et al. (2013). Determining the optimum grid-connected photovoltaic inverter size. Solar Energy, 87, 96–102.
[12] Kratzenberg, M. G., Deschamps, E. M., Nascimento, L., et al. (2014). Optimal photovoltaic inverter sizing considering different climate conditions and energy prices. Energy Procedia, 57, 226–235.
[13] Good, J., & Jeremiah, X. (2016). Impact of inverter loading ratio on solar photovoltaic system performance. Applied Energy, 177, 475–484.
[14] Mathur, A. S., Rajput, V. K., & Singh, B. P. (2025). Techno-economic feasibility and sensitivity analysis of a stand-alone solar photovoltaic power plant with battery energy storage using PVSyst. Next Research, 101015
[15] Shao, X., Zhang, Z., Zhang, Q., et al. (2021). Annual power generation gain model of bifacial photovoltaic modules based on PVsyst regression analysis. Acta Energiae Solaris Sinica, 42(1), 209.
[16] Pillai, D. S., Bayindir, A. B., Thiruchutan, A., et al. (2026). A comprehensive review of CAPEX-driven LCOE optimization strategies for utility-scale PV systems. Solar Energy, 306, 114296.
[17] Ibrahim, N. A., Alwi, S. R. W., Abd Manan, Z., Mustaffa, A. A., & Kidam, K. (2024). Climate change impact on solar system in Malaysia: Techno-economic analysis. Renewable and Sustainable Energy Reviews, 189, 113901